Hindawi
Shock and Vibration
Volume 2023, Article ID 6673458, 13 pages
https://doi.org/10.1155/2023/6673458

Research Article

Study on the Support Effect of Energy-Absorbing Support Structure in the Coal Mine Roadway and the Synergic Effect with Wall Rock

Shuwen Wang,[1] **Shijie Su**,[2] **Qian Zhao**,[2] **Dong An**,[3] **Yonghui Xiao**,[4] **and Hailiang Xu**[3]

[1]*China Coal Energy Group Co., Ltd., Beijing, China*
[2]*Zhongtian Hechuang Energy Co., Ltd, Inner Mongolia, China*
[3]*School of Civil Engineering, North China University of Technology, Beijing, China*
[4]*School of Physics, Liaoning University, Shenyang, China*

Correspondence should be addressed to Dong An; andong@ncut.edu.cn

Received 28 March 2023; Revised 17 May 2023; Accepted 26 May 2023; Published 20 June 2023

Academic Editor: Antonio Giuffrida

This paper examines the effectiveness of energy absorption anti-impact support in protecting the coal mine roadway from rock burst and ensuring safe production. By establishing an ABAQUS numerical model of the support and wall rock, the mechanical behavior of the system under static and impact loads have been investigated. The analysis includes the deformation of the wall rock, plastic strain, plastic property, and damage range to evaluate the support effect and the synergistic effect with the wall rock. The findings indicate that compared to ordinary support, the energy absorption anti-impact support exhibits a 20.40% increase in maximum deformation, 4.74% increase in maximum stress, 66.67% decrease in maximum plastic strain, and 116.79% increase in maximum absorption energy. The wall rock also experiences a 2.91% increase in maximum deformation and 10.19% increase in maximum stress. These results suggest that energy absorption anti-impact support is effective in improving the anti-impact performance of the support and providing a certain level of protection to both the support and wall rock.

1. Introduction

In recent years, China's coal mining industry has shifted to deep mining due to the depletion of shallow coal resources, resulting in more complex formation conditions and an increased risk of rock burst accidents [1]. Most rock burst incidents occur in roadway, causing significant damage to the wall rock and posing a serious threat to the safety of personnel and equipment [2]. Rock support in burst-prone grounds needs to address a few additional designs [3]. The use of yielding support is a key component when designing a rock burst support system. To prevent and mitigate these disasters, energy-absorbing technology has become a research area in roadway rock burst prevention and reduction [4].

Various studies have been conducted to improve roadway stability and prevent rock burst accidents [5–8], including the use of high-strength support systems such as single hydraulic columns and portal hydraulic supports. The yielding cable bolt has also been studied [9, 10]. Coal pore structure will also be affected by other factors [11–13]. Those mentioned above follow the rock support guiding principles. There are also some new support theories [14, 15]. There are some prevention and control methods for mining working face [16–18]. While these supports can reduce the probability of rock burst incidents, they may not be effective in mitigating the large impact energy associated with some rock burst disasters. To address this issue, Jiang et al. [19] proposed the use of energy-absorbing materials [20], energy absorption, and anti-impact coupling support [21], which have been shown to be effective in preventing rock burst accidents. Based on the theory of support systems and the analysis of roadway wall rock [22], a design

principle for anti-impact support has been proposed, and the energy absorption anti-impact hydraulic support [23] has been developed and successfully applied in the field. In addition, a folded thin-walled device [24] has been proposed as an energy absorption core device and yielding hydraulic support, and its mechanical properties have been studied.

This paper proposes that the use of a roadway energy absorption anti-impact support structure can significantly improve the prevention and control of rock burst in coal mines. The support structure works in synergy with the wall rock to enhance its effectiveness. To establish a system model between the energy absorption anti-impact support and the wall rock, a numerical calculation method is used. The mechanical state of the support and wall rock combination system is analyzed under both static and impact loads, based on the vertical and horizontal deformation of the roadway, equivalent plastic strain, plastic property, and damage range. These research indicators are used to study the support effect of the energy-absorbing support and its synergistic effect with the wall rock in coal mine roadway.

2. Engineering Application

2.1. Energy Absorption Anti-Impact Support in Coal Mine Roadway. The roadway, which is supported by anchor mesh, anchor rods, anchor cables, hydraulic lifting sheds, and hydraulic support for rock burst prevention, adopts a semicircular arch section. The roadway anti-impact hydraulic support is installed within the range of 40 m–260 m of the advanced coal mining face and the support is implemented at a spacing of 3 m. The support base is buried in the floor, and tracks and belts are laid on the base. The hydraulic support adopts an energy absorption anti-impact device, which is shown in Figure 1. There was a mining earthquake event in 2016 which caused the mechanical pressure gauge on the column in the two hydraulic supports for rock burst prevention to burst and damage, but the wall rock supported by the anti-impact structure did not have obvious deformation and showed no signs of damage. This event had a certain impact on the roadway in the support area, but the energy absorption anti-impact structure effectively resisted the dynamic process of the wall rock triggered by this mining earthquake.

2.2. Geological Background. The tectonics is a westward inclined monoclinic structure without faults. The dip angle of the coal seam is 1–3°, with an average thickness of 4.72 m and a burial depth of approximately 680 m. The surface water system in the mine field is not developed, and there are no surface water bodies such as reservoirs and lakes.

According to the test results of the mechanical properties of the top and bottom slates of the coal seams, the top and bottom slates of each coal seam are mainly mudstone, sandy mudstone, and siltstone, followed by fine and medium sandstone. The compressive strength of coal samples is the lowest among all rock types, belonging to soft rock and fractured rock mass.

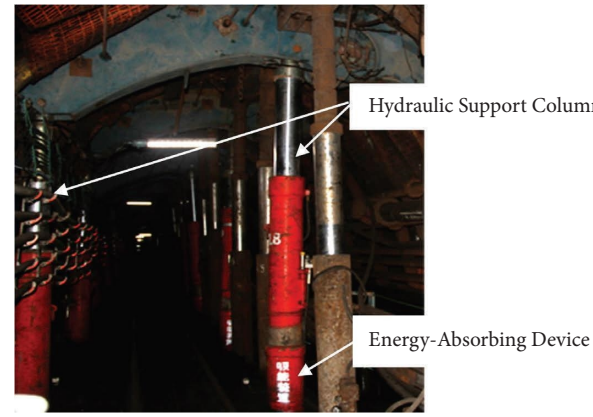

Figure 1: Photo of the roadway supported by the energy absorption anti-impact structure.

The compressive strength of the coal seam roof is between 3.20 MPa and 77.42 MPa, and the compressive strength of the coal sample belongs to soft rock with broken rock mass.

2.3. Energy-Absorbing Device. The crucial component of the energy absorption and anti-impact support is a structural member with special geometry [25, 26]. The mechanical properties and energy absorption effect of this member play a critical role in the anti-impact performance of the entire support. The main structure of this component is depicted in Figure 2.

The support function of the energy absorption anti-impact support depends on the deformation of the energy-absorbing device. After the deformation of the device, the support still has sufficient working resistance while allowing the limited deformation of the wall rock to continue to release energy, which can not only adapt to the deformation of the wall rock but also control the deformation of the wall rock, giving full play to the support effect of the support. Based on the abovementioned engineering applications, this paper studies the deformation synergy of the roadway wall rock support model.

3. Simulation Calculation

3.1. Simulation Model. The finite element model for this study was constructed using ABAQUS software, and the calculation model is depicted in Figure 3. The roadway has a width of 4.88 m. To minimize the boundary effects on the model calculation process, a range of 3–5 times the tunnel diameter is selected around the roadway and the model size is 30 m × 30 m × 0.5 m. The wall rock adopts the Mohr–Coulomb constitutive relationship, and the mechanical parameters are presented in Table 1.

The energy absorption anti-impact support is composed of Q550 steel with a yield strength of 550 MPa, a density of 7850 kg/m^3, an elastic modulus of 206 GPa, and Poisson's ratio of 0.3. The simulation process adopts an ideal elastoplastic constitutive model, without considering the hardening properties of the steel. The entire model uses

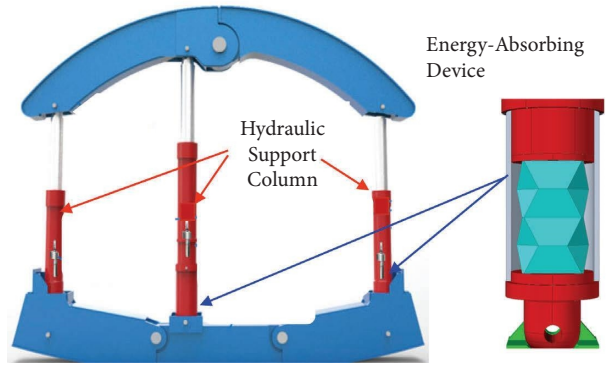

Figure 2: Energy absorption anti-impact support.

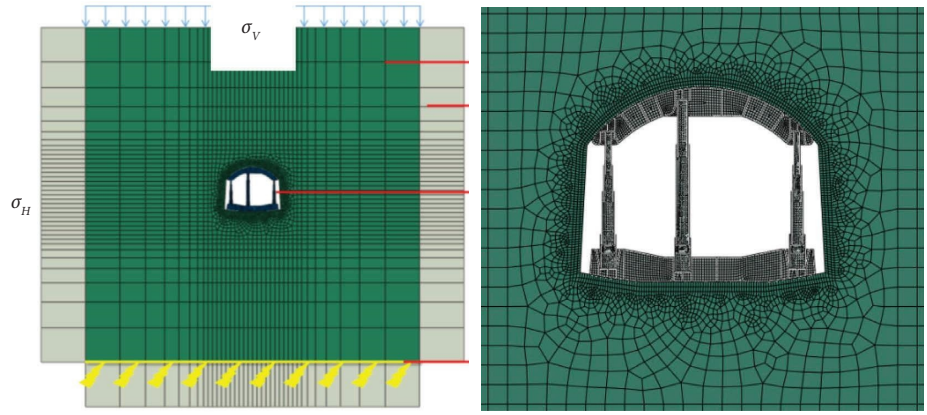

Figure 3: Roadway wall rock support model.

universal contact, with normal behavior defined as "hard contact," tangential behavior defined as a penalty function, and a friction coefficient of 0.3. The wall rock element type is C3D8R, with a total of 8288 elements, while the rack unit type is S4R, with a total of 14456 units. Infinite elements are used around and at the bottom of the model, and the element type is CIN3D8. The method of coupling the finite element and infinite element is used to simulate the surrounding infinite space.

3.2. Calculation Condition. To investigate the difference in support effectiveness between the energy-absorption anti-impact support and ordinary support without an energy-absorbing device, a comparison working condition was established. Vertical stress is simulated for the upper part of the wall rock, while horizontal stress adopts different lateral pressure coefficients.

Two stress ratios were applied to load the wall rock, and the specific calculation working conditions are presented in Table 2.

4. Simulation Results

4.1. Support Deformation. The support deformation in the roadway for each working condition is shown in Figure 4, while the maximum value of support deformation is presented in Table 3.

Based on the results shown in Figure 4 and Table 3, it can be observed that the energy absorption support deformation increased by 20.40% compared to the ordinary support, with the maximum deformation occurring at the upper right column. In addition, the anti-impact support exhibits the characteristic of deformation giving way to the overall deformation compared to the ordinary support. When the ordinary support is subjected to external impact, the deformation is biased to one side, and the column displacement is larger when the load increases. Although the deformation of the top beam down and bottom beam up of the energy absorption anti-impact support is larger than that of the ordinary support, the integrity is better, and the column part is close to the overall translation to ensure a "strong column" [27]. Therefore, to further compare the support deformation in the vertical direction under different working conditions, the vertical support deformation is analyzed.

Figure 5 illustrates the vertical deformation of the supports. With the energy-absorbing device added at the bottom of the hydraulic column, the vertical displacement of the entire energy-absorption anti-impact support is primarily the rigid displacement of the bottom beam. In contrast, the vertical displacement of the column is small. This demonstrates that the energy-absorbing device plays a crucial role in protecting the column and preventing it from bending damage.

Table 1: Mechanical parameters of strata and rock.

	Thickness (m)	Density (kg/m^3)	Bulk modulus (GPa)	Shear modulus (GPa)	Tensile strength (MPa)	Cohesion (MPa)	Internal friction angle (°)
Coarse sandstone	0.5	2540	14.7	8.1	11.55	10.0	45

Table 2: Calculation working conditions.

$\sigma_H = 10$ MPa	$\sigma_V = 10$ MPa	$\sigma_V = 20$ MPa
Ordinary support	1	2
Energy absorption support	3	4

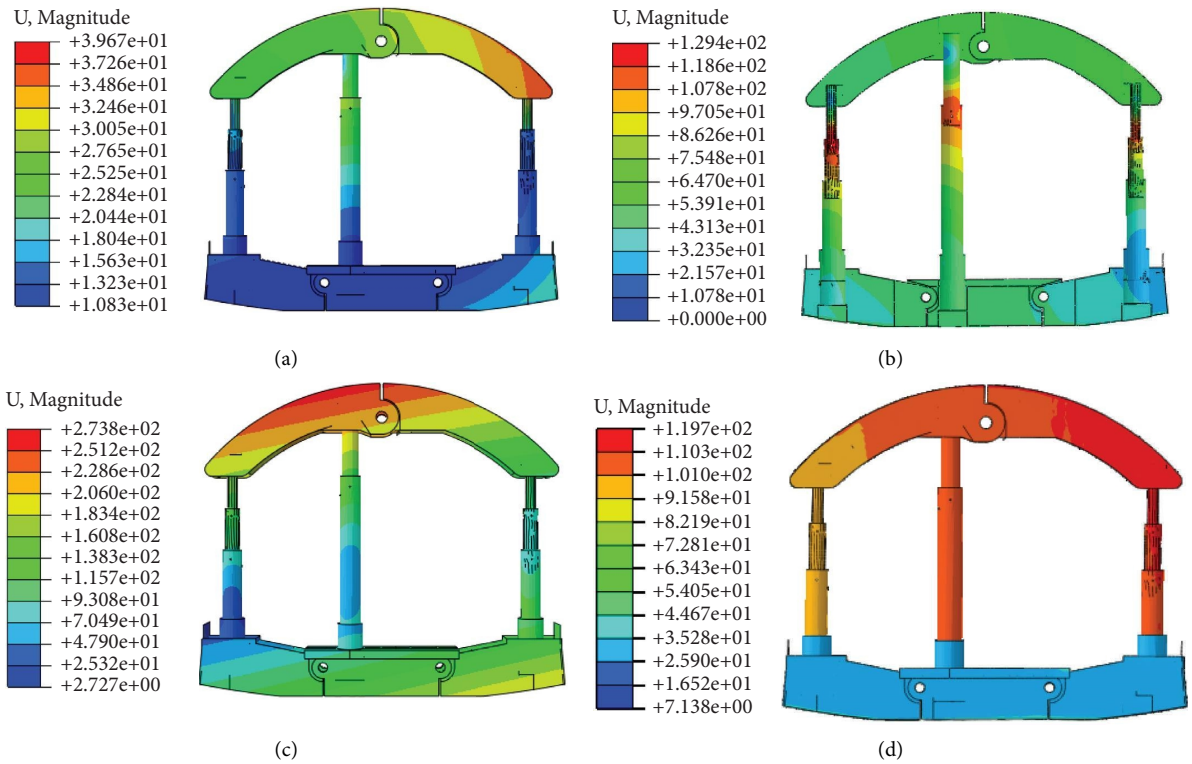

Figure 4: Support deformation diagram: (a) work condition 1, (b) work condition 2, (c) work condition 3, and (d) work condition 4.

Table 3: Support deformation.

$\sigma_H = 10$ MPa	$\sigma_V = 10$ MPa (mm)	$\sigma_V = 20$ MPa (mm)
Ordinary support	39.67	129.40
Energy absorption support	59.70	155.80

4.2. Support Stress and Damage Range. The stress of the support is shown in Figure 6. The maximum value of stress is shown in Table 4.

For ordinary supports, the stress is mainly concentrated in the upper part of the three columns and the connection between the middle column and the top beam. When the vertical load increases to 20 MPa, the stress is mainly concentrated in the upper part of the three columns and the variable cross section of the left and right columns. For the energy absorption anti-impact support, the stress compared with the ordinary support stress, it increased by 4.74%, mainly concentrated in the upper part of the left and right columns. Compared with the ordinary support stress, energy absorption devices are mainly concentrated in the bottom beam which increased by 9.09%. The upper left and right column strengths of both brackets are low, and there is a risk of yielding during application. After the energy-absorbing device is applied to the support, the stress in the upper part of the center column is obviously reduced, the overall stress distribution is more uniform, the stress concentration parts are reduced, and the support is more reasonably stressed.

The equivalent plastic strain of the supports is shown in Figure 7. The maximum values of the equivalent plastic strain are shown in Table 5.

The energy absorption anti-impact support is adopted, and the overall stress of the support is different from the position of the maximum equivalent plastic strain of the ordinary support. The maximum equivalent plastic strain of the ordinary support occurs at the location of the mid-column variable cross section, whose place is more dangerous. The maximum equivalent plastic strain of the energy absorption anti-impact support occurs at the position of the limit hinge of the bottom beam, and compared with the ordinary support, the plastic strain decreased by 66.67%. In the actual production and application process, there is thickening treatment at the position of the limit hinge, and it

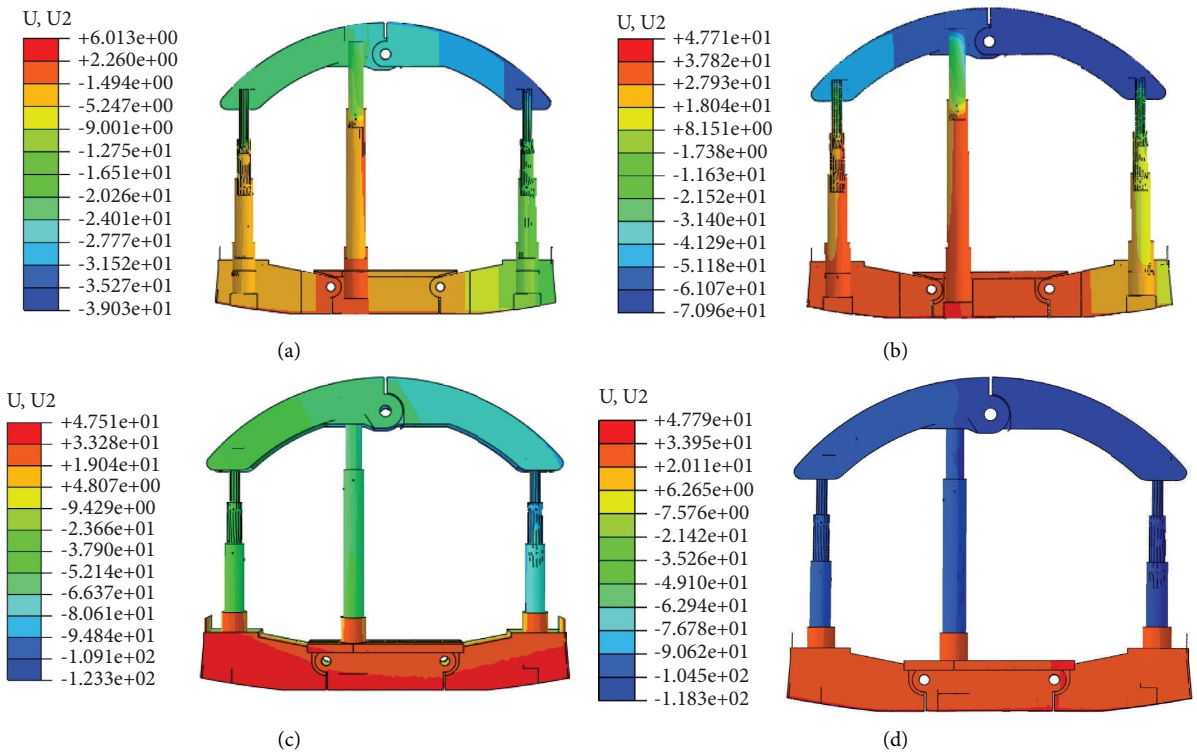

Figure 5: Support vertical deformation diagram: (a) work condition 1, (b) work condition 2, (c) work condition 3, and (d) work condition 4.

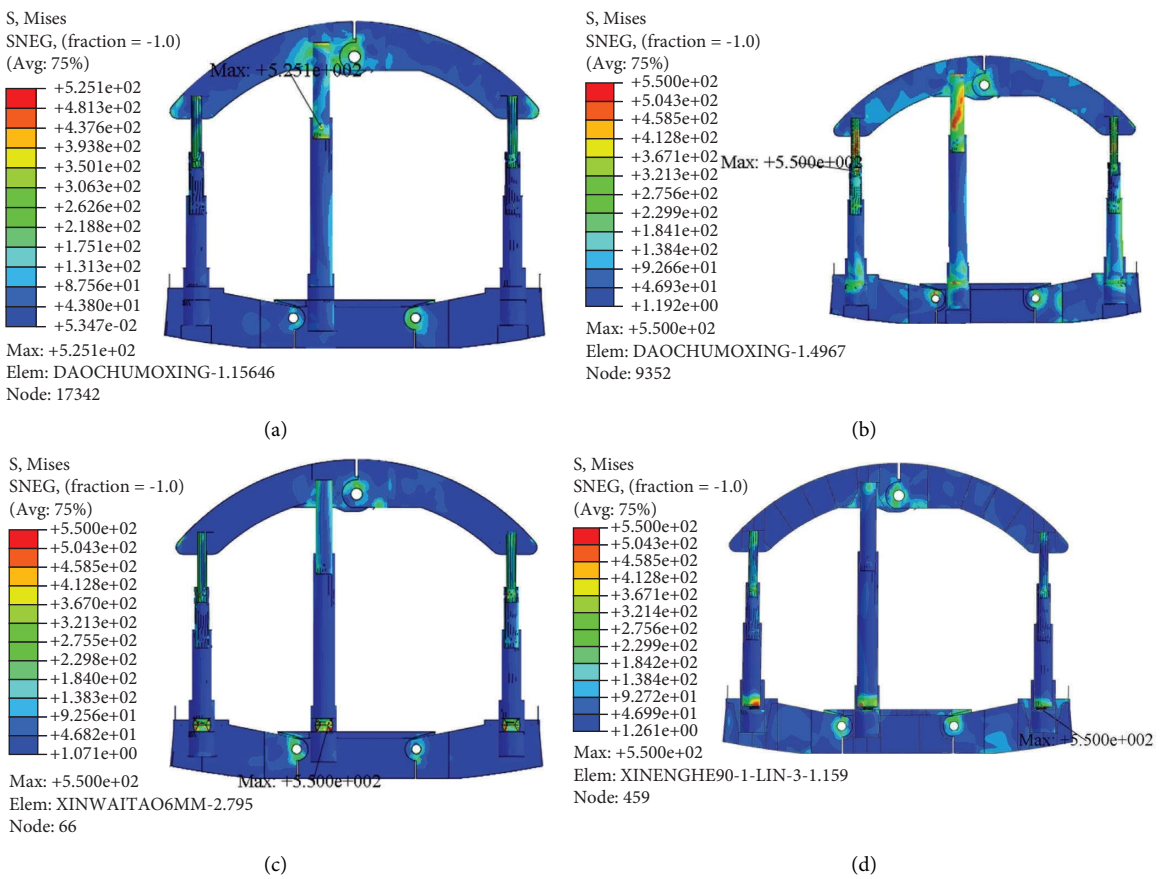

Figure 6: Support stress diagram: (a) work condition 1, (b) work condition 2, (c) work condition 3, and (d) work condition 4.

Table 4: Support stress.

$\sigma_H = 10$ MPa	$\sigma_V = 10$ MPa	$\sigma_V = 20$ MPa
Ordinary support	525.10	550.00
Energy absorption support	550.00	600.00

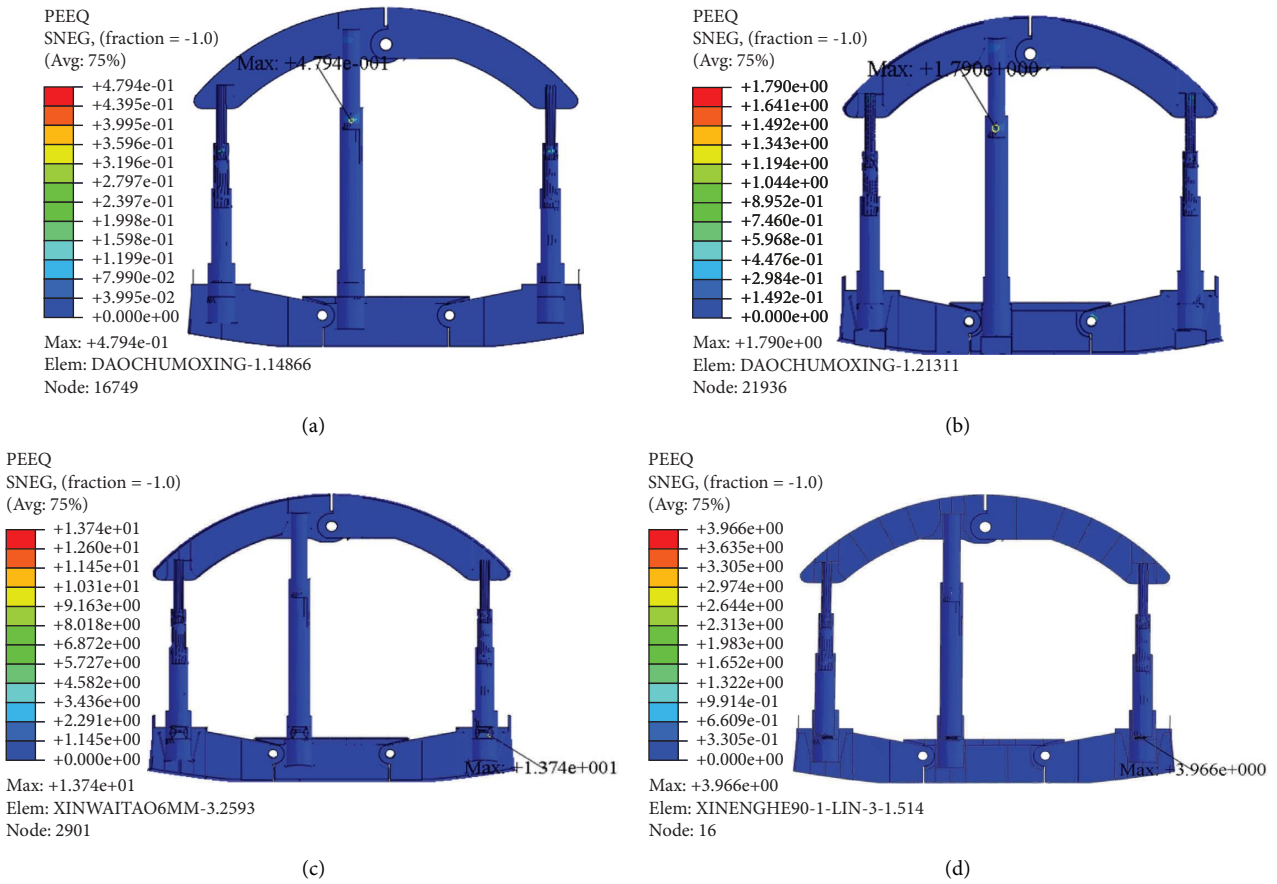

Figure 7: Equivalent plastic strain of the support: (a) work condition 1, (b) work condition 2, (c) work condition 3, and (d) work condition 4.

Table 5: Equivalent plastic strain.

$\sigma_H = 10$ MPa	$\sigma_V = 10$ MPa	$\sigma_V = 20$ MPa
Ordinary support	0.48	1.79
Energy absorption support	0.16	0.56

can be considered that the position meets the safety requirements.

The plastic strain distribution of the support is shown in Figure 8. Plastic deformation occurs in the upper part of the three columns of the ordinary support, while the columns of energy absorption anti-impact support are still within the elastic range of the line. Therefore, it can be considered that the energy-absorbing device applied in the support can play a good role in protecting the support, making the force of the whole support more uniform and reasonable, and favorably reducing the risk of damage to the support.

4.3. Support Energy. The energy nephogram of the three columns of the support under each working condition is shown in Figure 9. The energy absorbed is shown in Table 6. It can be observed that the energy absorption is more than twice that of ordinary support. The energy absorption of the three columns is not equal, and the most energy absorbed place is the left column. The energy absorption of the middle column is the average of the left and right columns. When the entire support is impacted, due to the close distance between the left two columns, it bears more energy absorption function, while the right column absorbs less energy. The support structure can be optimized in the future.

4.4. Wall Rock Deformation. The deformation of the wall rock is shown in Figure 10. Compared with the ordinary support, when the wall rock is with the energy absorption support, its deformation is improved by 3.59% and 2.91%, respectively. It can be considered that the energy absorption

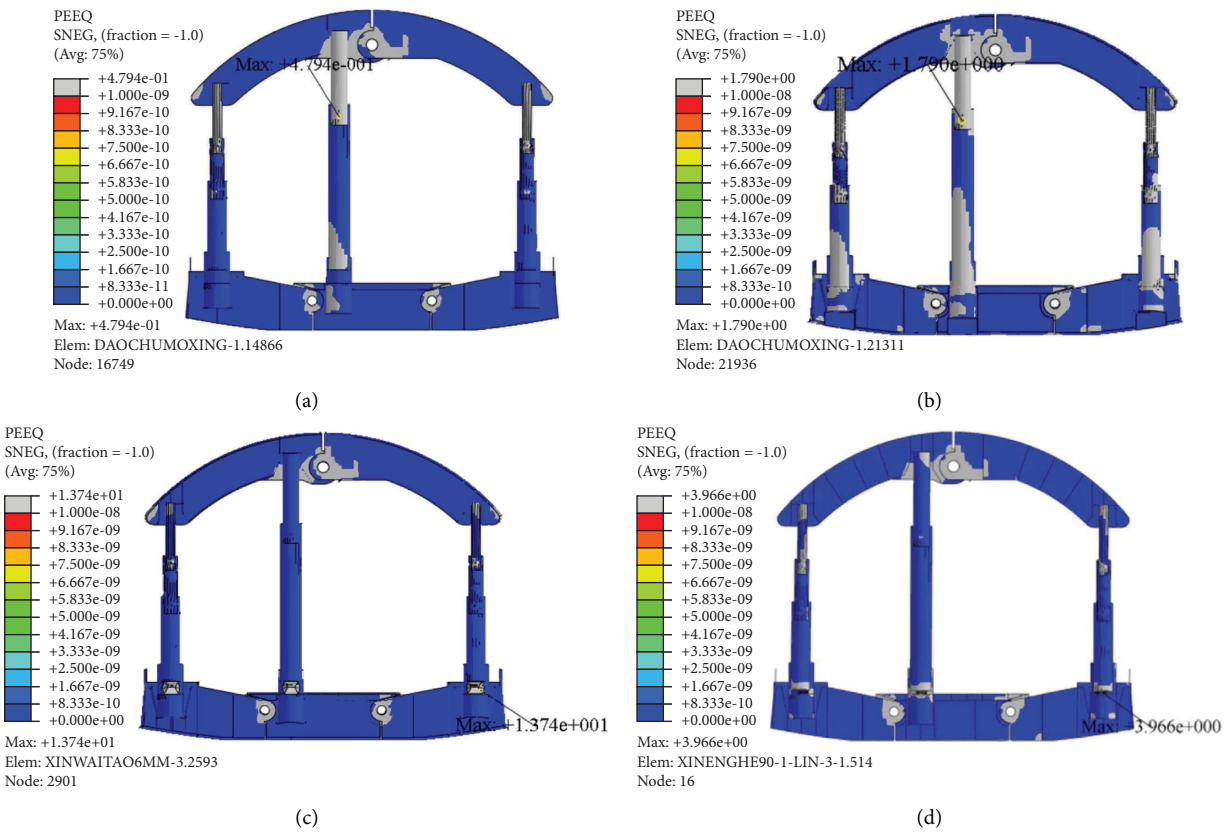

Figure 8: Plastic strain distribution of the support: (a) work condition 1, (b) work condition 2, (c) work condition 3, and (d) work condition 4.

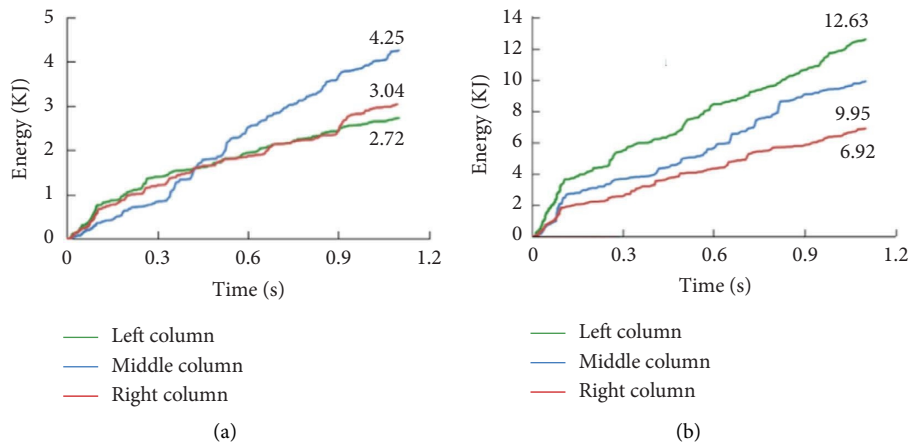

Figure 9: Continued.

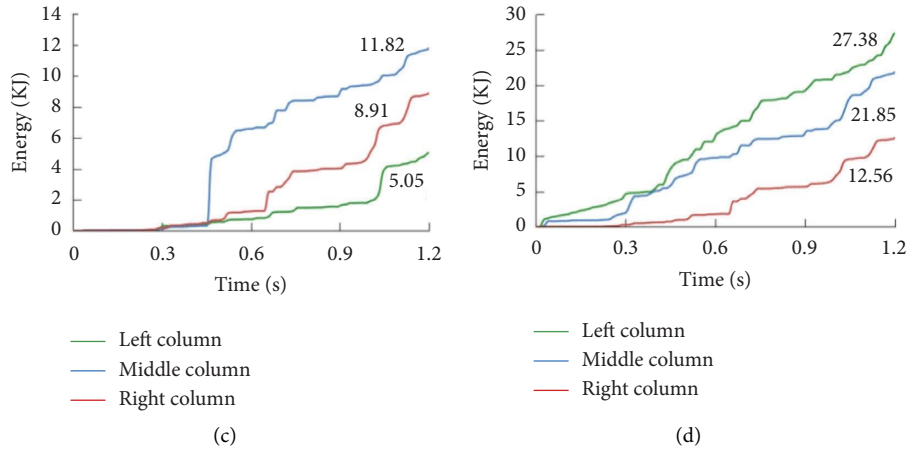

Figure 9: Energy nephogram of the support: (a) work condition 1, (b) work condition 2, (c) work condition 3, and (d) work condition 4.

Table 6: Equivalent plastic strain of column.

$\sigma_H = 10$ MPa		$\sigma_V = 10$ MPa	$\sigma_V = 20$ MPa
Ordinary support	Left	4.25	12.63
	Middle	3.04	9.95
	Right	2.72	6.92
Energy-absorption support	Left	11.82	27.38
	Middle	8.91	21.85
	Right	5.05	12.56

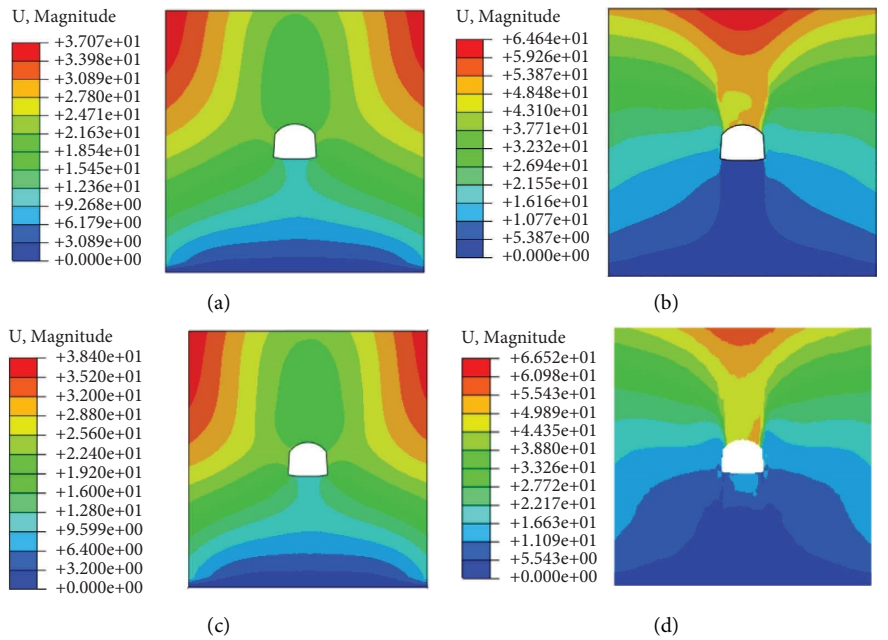

Figure 10: Wall rock deformation: (a) work condition 1, (b) work condition 2, (c) work condition 3, and (d) work condition 4.

anti-impact support is used to give way first and then resist to the wall rock, which can also ensure the overall deformation of the wall rock.

The energy absorption anti-impact support calculated in this paper has a yielding effect in the vertical direction. From the vertical deformation of the wall rock in Figure 11,

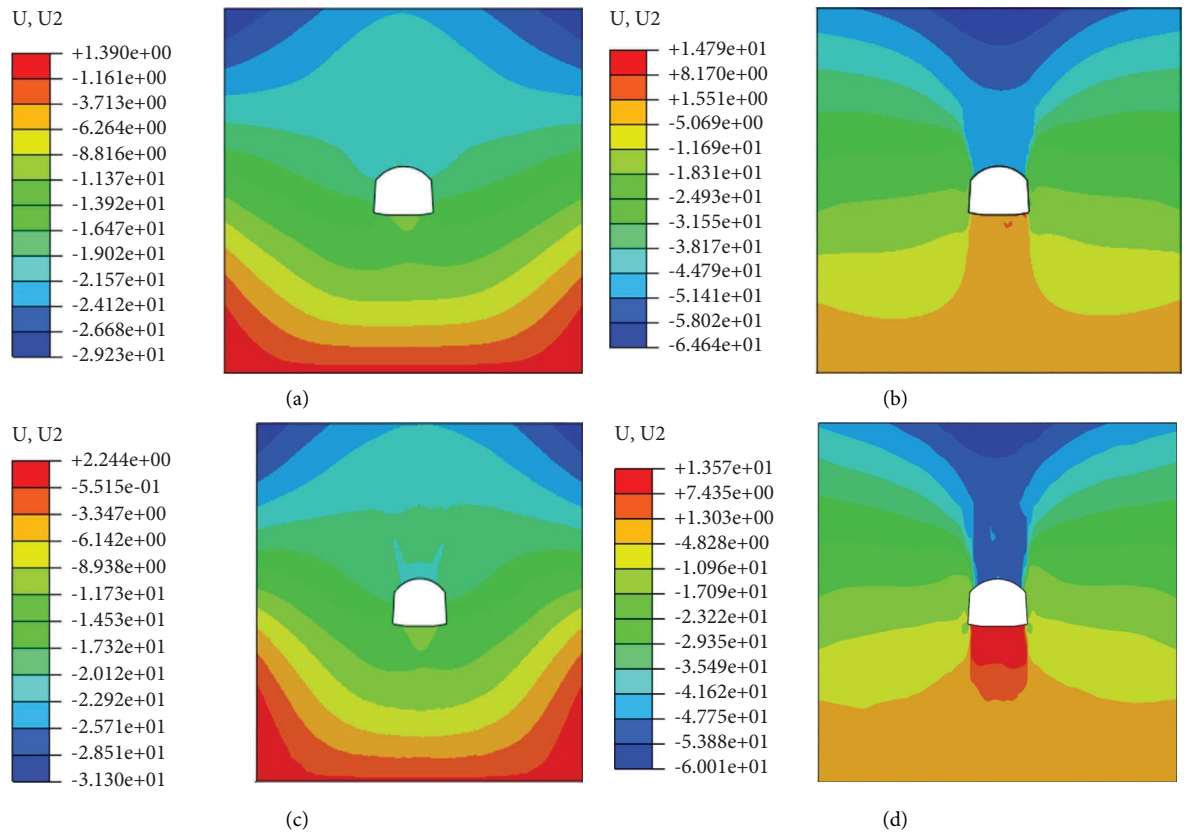

Figure 11: Vertical deformation of the wall rock: (a) work condition 1, (b) work condition 2, (c) work condition 3, and (d) work condition 4.

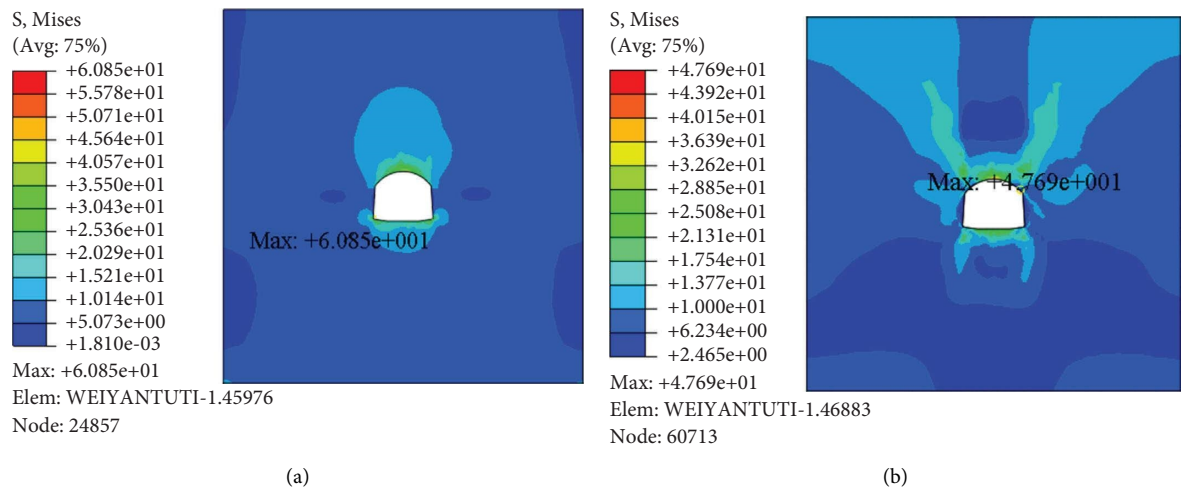

Figure 12: Continued.

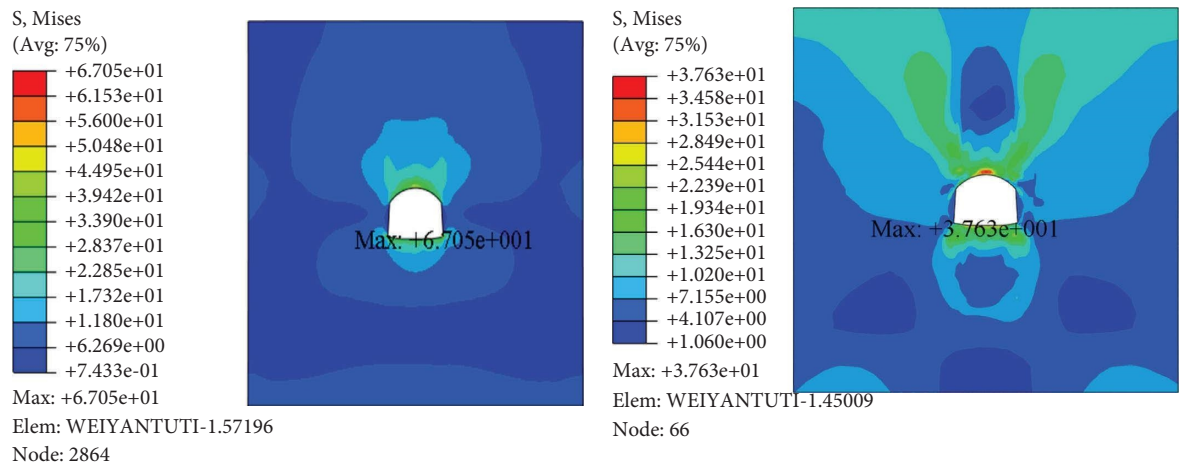

Figure 12: Mises stress of the wall rock: (a) work condition 1, (b) work condition 2, (c) work condition 3, and (d) work condition 4.

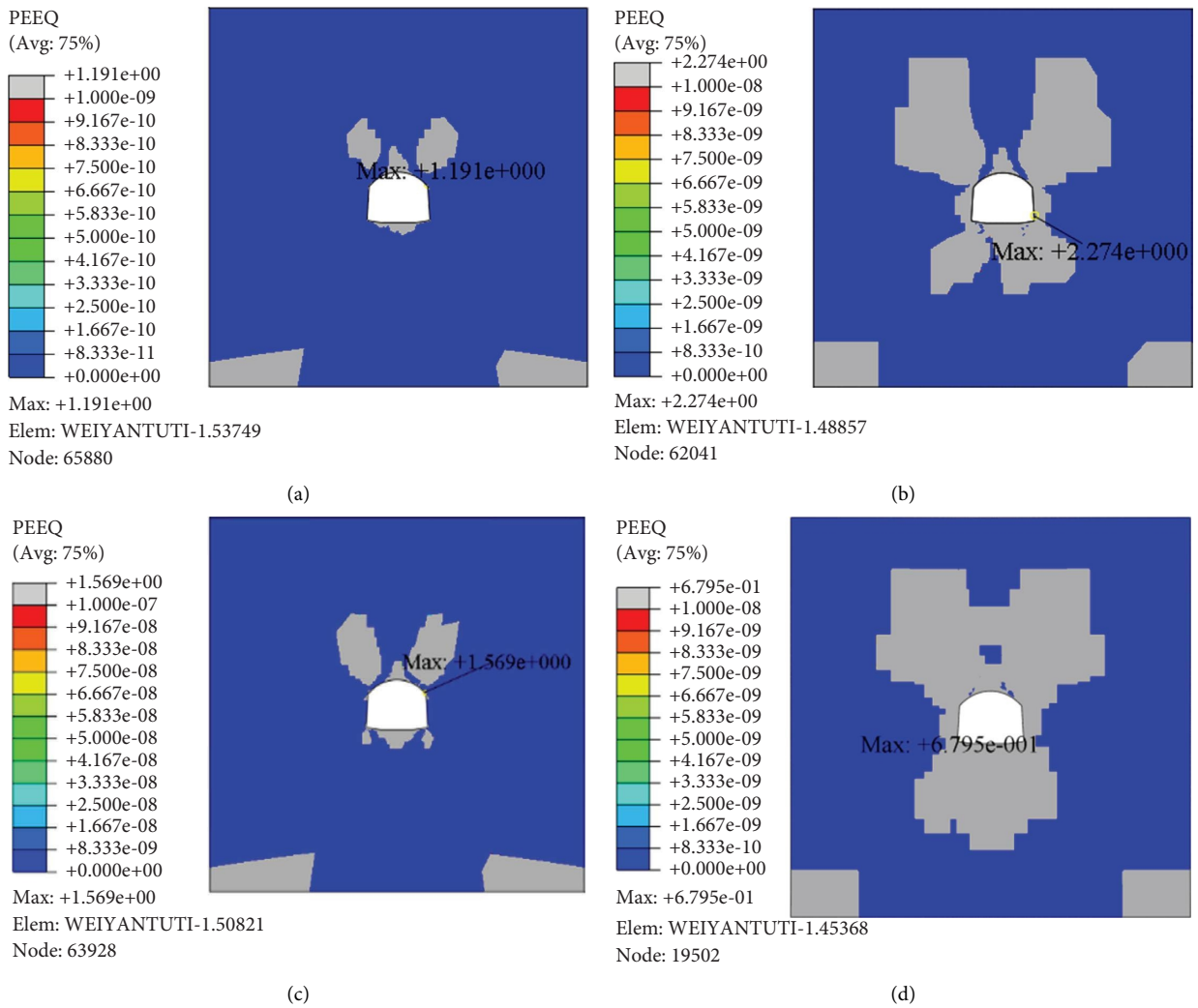

Figure 13: Equivalent plastic strain distribution of the wall rock: (a) work condition 1, (b) work condition 2, (c) work condition 3, and (d) work condition 4.

because the energy absorption anti-impact support leaves a deformation space of about 120 mm in the vertical direction, when the external force acts on the support, the allowable deformation is larger compared to the ordinary support. Finally, the deformation in the vertical direction of the wall rock increases when the wall rock is supported by the energy absorption anti-impact support, and the maximum value only increases by 0.85 mm. That means the energy-absorbing device applied in the roadway, the wall rock, and the energy absorption anti-impact support can deform together. The support first gives way, the wall rock resists the external impact, and then the support and the wall rock resist the pressure together to achieve synergy.

4.5. Wall Rock Stress and Damage Range. The stress distribution in the wall rock is shown in Figure 12. In the process of deformation of the energy absorption anti-impact support giving way, the wall rock stress has a certain degree of release, making the secondary stress redistribution process also increase the scope of influence. Compared with the ordinary support, the maximum stress of the wall rock is increased when the energy absorption anti-impact device supports the wall rock; when $\sigma_H = 10$ MPa and $\sigma_V = 10$ MPa, the maximum stress is 67.05 MPa and the maximum value is increased by 10.19%, and when $\sigma_H = 10$ MPa and $\sigma_V = 20$ MPa, the maximum stress is 55.52 MPa and the maximum value is increased by 16.42%. The equivalent plastic strain distribution of the wall rock for each working condition is shown in Figure 13. The plastic zone of the wall rock is increased when the energy-absorbing device is used, making full use of the wall rock itself to resist external dynamic loads.

5. Conclusion

(1) After the energy-absorbing support mentioned in this article was used in a certain project, a mining earthquake occurred in a coal mine. The mechanical part of the hydraulic support column was damaged due to excessive pressure, but the deformation of the wall rock roadway was not significant, and the support structure did not show any damage. The energy-absorbing and anti-impact support effectively resisted the dynamic damage of the wall rock caused by the mining earthquake.

(2) The addition of the energy-absorbing device in the support has significant advantages. The stress concentration area is reduced, and the overall stress distribution becomes more uniform. This results in a more reasonable stress distribution on the support and reduces the risk of damage. The energy-absorbing device also allows for deformation giving way to the overall deformation, making the force of the whole support more uniform and reasonable. Therefore, the energy-absorbing device applied in the support plays a significant role in protecting the support.

(3) The energy absorption anti-impact support can effectively absorb more energy compared to ordinary support. This means that it can reduce the plastic damage caused by the impact load on the hydraulic support. This feature is particularly useful in environments where impact loads are high, as it can help prevent structural damage and ensure the long-term stability of the support.

(4) The energy absorption anti-impact support can deform together with the wall rock. This means that the support first gives way, and then the wall rock resists external shocks, and finally, the support and the wall rock resist pressure together. This process achieves synergy between the support and the wall rock, ensuring the overall deformation of the wall rock. The energy absorption anti-impact support's ability to give way first and then resist the wall rock makes it an excellent choice for supporting the tunnel structure in environments where impact loads are high.

Data Availability

The data used to support the findings of this study are included within the article.

Conflicts of Interest

The authors declare that there are no conflicts of interest.

Acknowledgments

This work was supported by the Joint Major Funds of the National Natural Science Foundation of China and Liaoning (U1908222) and the Major Science and Technology Projects of China National Coal Group (20211BY001).

References

[1] M. C. He, H. P. Xie, S. P. Peng, and Y. D. Jiang, "Study on rock mechanics in deep mining engineering," *Chinese Journal of Rock Mechanics and Engineering*, vol. 16, pp. 2803–2813, 2005.

[2] Y. S. Pan, Z. H. Li, and M. Z. Zhang, "Distribution, type, mechanism, and prevention of rockburst in China," *Chinese Journal of Rock Mechanics and Engineering*, vol. 22, no. 11, pp. 1844–1851, 2003.

[3] M. Cai, "Principles of rock support in burst-prone ground," *Tunnelling and Underground Space Technology*, vol. 36, pp. 46–56, 2013.

[4] K. X. Wang and Y. S. Pan, "An undified theory of energy absorption and anti-impact for wall rock and support in rock burst mine," *Rock and Soil Mechanics*, vol. 9, pp. 2585–2590, 2015.

[5] J. Lv, L. Wang, L. L. Liu, and W. L. Sun, "Study on comprehensive support performance of constant resistance and large deformation anchor cable and single hydraulic support," *Coal Mine Machinery*, vol. 41, no. 09, pp. 45–48, 2020.

[6] W. J. Xu and H. J. Gu, "Heighten of rock burst performance of hydraulic support in mine," *Coal Technology*, vol. 28, no. 09, pp. 23-24, 2009.

[7] Y. Zhang, J. Wang, H. Y. Wei, and W. F. Fan, "Study on temporary portal type support technology in impact area of

roof cutting by gob-side entry retaining," *Coal Science and Technology*, vol. 46, no. S1, pp. 23–26+38, 2018.

[8] H. L. Xu, X. Guo, Y. M. Song, J. Q. Song, and D. An, "Research on synergistic action system of energy-absorbing demising anti-impact support structure and wall rock," *Journal of Safety Science and Technology*, vol. 17, no. 12, pp. 111–116, 2021.

[9] W. Wang, Y. S. Pan, and Y. H. Xiao, "Synergistic resin anchoring technology of rebar bolts in coal mine roadways," *International Journal of Rock Mechanics and Mining Sciences*, vol. 151, Article ID 105034, 2022.

[10] W. Wang, Y. S. Pan, and Y. H. Xiao, "Synergistic mechanism and technology of cable bolt resin anchoring for roadway roofs with weak interlayers," *Rock Mechanics and Rock Engineering*, vol. 55, no. 6, pp. 3451–3472, 2022.

[11] S. M. Liu and X. L. Li, "Experimental study on the effect of cold soaking with liquid nitrogen on the coal chemical and microstructural characteristics," *Environmental Science and Pollution Research*, vol. 30, no. 13, pp. 36080–36097, 2022.

[12] S. M. Liu, H. T. Sun, D. M. Zhang et al., "Nuclear magnetic resonance study on the influence of liquid nitrogen cold soaking on the pore structure of different coals," *Physics of Fluids*, vol. 35, no. 1, Article ID 012009, 2023.

[13] S. M. Liu, H. T. Sun, D. M. Zhang et al., "Experimental study of effect of liquid nitrogen cold soaking on coal pore structure and fractal characteristics," *Energy*, vol. 275, no. 7, Article ID 127470, 2023.

[14] M. S. Gao, Y. L. He, D. Xu, and X. Yu, "A new theoretical model of rock burst-prone roadway support and its application," *Geofluids*, vol. 2021, Article ID 5549875, 11 pages, 2021.

[15] W. J. Liu, D. Y. Qian, X. G. Yang et al., "Stress relief and support for stability of deep mining roadway with thick top coal in hujiahe coal mine with the risk of rock burst," *Shock and Vibration*, vol. 2021, Article ID 3822336, 16 pages, 2021.

[16] L. B. Zhang, W. L. Shen, X. L. Li et al., "Abutment pressure distribution law and support analysis of super large mining height face," *International Journal of Environmental Research and Public Health*, vol. 20, no. 1, p. 227, 2022.

[17] X. L. Li, X. Y. Zhang, W. L. Shen et al., "Research on the mechanism and control technology of coal wall sloughing in the ultra-large mining height working face," *International Journal of Environmental Research and Public Health*, vol. 20, no. 1, p. 868, 2023.

[18] J. C. Zhang, X. L. Li, Q. Qin, Y. Wang, and X. Gao, "Study on overlying strata movement patterns and mechanisms in super-large mining height stopes," *Bulletin of Engineering Geology and the Environment*, vol. 82, no. 4, p. 142, 2023.

[19] Y. D. Jiang, Y. S. Pan, F. X. Jiang, L. M. Dou, and Y. Ju, "State of the art review on mechanism and prevention of coal bumps in China," *Journal of China Coal Society*, vol. 39, no. 02, pp. 205–213, 2014.

[20] S. C. K. Yuen and G. N. Nurick, "The energy-absorbing characteristics of tubular structures with geometric and material modifications: an overview," *Applied Mechanics Reviews*, vol. 61, no. 2, Article ID 020802, 2008.

[21] Y. S. Pan, X. F. Lv, and Z. H. Li, "The model of energy-absorbing coupling support and its application in rock burst roadway," *Journal of Mining & Safety Engineering*, vol. 28, no. 01, pp. 6–10, 2011.

[22] Q. Li, H. Wang, Y. S. Pan, H. Luo, and W. H. Zheng, "Roadway supporting wall rock system dynamic responses under impact load," *Journal of Liaoning Technical University*, vol. 33, no. 02, pp. 213–217, 2014.

[23] Y. S. Pan, Y. H. Xiao, and G. Z. Li, "Roadway hydraulic support for rockburst prevention in coal mine and its application," *Journal of China Coal Society*, vol. 45, no. 01, pp. 90–99, 2020.

[24] Y. S. Pan, Y. H. Xiao, G. Z. Li, and K. X. Wang, "Study of tunnel support theory of rockburst in coal mine and its application," *Journal of China Coal Society*, vol. 39, no. 2, pp. 222–228, 2014.

[25] D. An, T. Liu, H. Cui, Z. Chen, H. Xu, and Y. Song, "Study of the factors influencing load displacement curve of energy absorbing device by area division simulation," *Scientific Reports*, vol. 12, no. 1, Article ID 13492, 2022.

[26] Y. M. Song, H. Ren, H. L. Xu, X. Guo, Z. Chen, and D. An, "Study on synergistic system of energy-absorbing yielding anti-impact supporting structure and surrounding rock," *Scientific Reports*, vol. 12, no. 1, p. 594, 2022.

[27] Y. L. Feng, J. Wu, X. Zhong, and S. P. Meng, "Damage concentration effect analysis of buckling-restrained braced frames after yielding of the braces," *China Civil Engineering Journal*, vol. 52, no. 06, pp. 45–54, 2019.